

Equilibrium distributions in a thermodynamical traffic gas

Milan Krbálek

Faculty of Nuclear Sciences and Physical Engineering, Czech Technical University,
Trojanova 13, 120 00 Prague, Czech Republic

Received 24 October 2006, in final form 11 April 2007

Published 14 May 2007

Online at stacks.iop.org/JPhysA/40/5813

Abstract

We derive the exact formula for thermal-equilibrium spacing distribution of a one-dimensional particle gas with a repulsive potential $V(r) = r^{-\alpha}$ ($\alpha > 0$) depending on the distance r between the neighbouring particles. The calculated distribution (for $\alpha = 1$) is successfully compared with the highway-traffic clearance distributions, which provides a detailed view of changes in the microscopical structure of a traffic sample depending on the traffic density. In addition to that, the observed correspondence is a strong support of studies applying the equilibrium statistical physics to traffic modelling.

PACS numbers: 05.70.-a, 05.20.-y, 45.70.Vn

(Some figures in this article are in colour only in the electronic version)

Investigation of one-dimensional particle ensembles seems actually to be very useful for understanding the complex system called *vehicular traffic*. Besides the favourite cellular automata, in the recent time a new trend appears in traffic modelling. Application of the equilibrium statistical physics to traffic ensembles (queuing systems of spatially interacting particles) has been many times discussed (see for example [2] and other references therein) and successfully demonstrated in articles [5, 9] and [7]. It has been manifested in [9] that the thermodynamics approach can be applied to such a many-particle-driven system as traffic flow, based on a microscopic description, in analogy with equilibrium physical systems. Besides, it has been demonstrated in [7] that the relevant statistical distributions obtained from the local thermodynamical model are in accord with those from traffic data measured on real freeways by the induction-loop detectors. It opens up an opportunity for finding the analytical form of probability density for clear distance among the cars (i.e., *clearance distribution* in traffic terminology) moving in traffic stream. Up to now the question about analytical form of clearance distribution has only been a subject of speculations (see the [2, 6])—never successfully answered.

We aim to use the one-dimensional thermodynamical particle gas to the prediction of a microscopical structure in traffic flows and consequently make a comparison to the relevant traffic data distributions. Justification for the approach described can be found in [5] and

[3] where it is proved that the equilibrium solution of a certain family of the particle gases (exposed to the heat bath with the temperature $T \geq 0$) is a good approximation for steady-state solution of driven many-particle systems with asymmetrical interactions. Since the vehicular traffic is a dissipative system of active elements (moving far from equilibrium), it is evident (see [9] and [5]) that thermodynamics-balance approach can be used on a mesoscopic level only (i.e., for small-sized samples of N vehicles), where the traffic density fluctuates around the constant value and distances and velocities are mutually uncorrelated. Then the stationary solution of the relevant Fokker–Planck equation practically coincides with the thermal-balance probability density of a certain statistical gas (see [5]). Moreover, the possibility for using the thermodynamical approach is supported by the fact that distribution of velocities in traffic sample fully corresponds to the Gaussian distribution (in each traffic-density interval)—see [2, 4], and [7]. Overall, it is sufficiently justified that traffic systems can be *locally* (i.e., on a mesoscopic level) described by instruments of equilibrium statistical physics.

Thus, consider N identical particles (vehicles) on the circumference $L = N$ of a circle. Let x_i ($i = 1, \dots, N$) denote the circular position of the i th particle. Put $x_{N+1} = x_1 + 2\pi$, for convenience. Now we introduce the short-ranged potential energy

$$U \propto \sum_{i=1}^N V(r_i),$$

where $V(r_i)$ corresponds to the repulsive two-body potential depending on the distance $r_i = |x_{i+1} - x_i| \frac{N}{2\pi}$ between the neighbouring particles only. Nearest-neighbour interaction is chosen with respect to the realistic behaviour of the car driver in traffic sample (see [7]). Besides, the potential $V(r)$ has to be defined so that $\lim_{r \rightarrow 0^+} V(r) = \infty$ which prevents particles passing through each other. The Hamiltonian of the described ensemble reads as

$$\mathcal{H} = \frac{1}{2} \sum_{i=1}^N (v_i - \bar{v})^2 + C \sum_{i=1}^N V(r_i),$$

with v_i being the i th particle velocity and C the positive constant. Note that \bar{v} represents the mean velocity in the ensemble. Then, the appropriate partition function¹

$$\mathcal{Z} = \int_{\mathbb{R}^{2N}} \delta\left(L - \sum_{i=1}^N r_i\right) \prod_{i=1}^N \exp\left(-\frac{(v_i - \bar{v})^2}{2\sigma^2}\right) \exp\left(-C \frac{V(r_i)}{\sigma^2}\right) dr_i dv_i \quad (1)$$

leads us (after $2N - 1$ integrations) to the simple assertion that the velocity v of particles is Gaussian distributed, i.e.

$$P(v) = \frac{1}{\sqrt{2\pi}\sigma} \exp\left(-\frac{(v - \bar{v})^2}{2\sigma^2}\right)$$

is the corresponding probability density.

Of larger interest, however, is the spacing distribution $P_\beta(r)$. To calculate the exact form of $P_\beta(r)$ one can restrict the partition function (1) by N velocity integrations to the reduced form

$$\mathcal{Z}_N(L) = \int_{\mathbb{R}^N} \delta\left(L - \sum_{i=1}^N r_i\right) \exp\left(-\beta \sum_{i=1}^N V(r_i)\right) dr_1 \dots dr_N,$$

where $\beta = C\sigma^{-2}$ is the *inverse temperature* (dimensionless) of the heat bath. Denoting $f(r) = e^{-\beta V(r)}$ the previous expression changes to

$$\mathcal{Z}_N(L) = \int_{\mathbb{R}^N} \delta\left(L - \sum_{i=1}^N r_i\right) \prod_{i=1}^N f(r_i) dr_1 \dots dr_N.$$

¹ σ is the constant representing a statistical variance.

Applying the Laplace transformation (see the [1] for details) one can obtain

$$g_N(p) \equiv \int_0^\infty \mathcal{Z}_N(L) e^{-pL} dL = \left(\int_0^\infty f(r) e^{-pr} dr \right)^N \equiv [g(p)]^N.$$

Then the partition function (in the large N limit) can be computed with the help of the Laplace inversion

$$\mathcal{Z}_N(L) = \frac{1}{2\pi i} \int_{B-i\infty}^{B+i\infty} g_N(p) e^{Lp} dp.$$

Its value is well estimated by the approximation in the saddle point B which is determined using the equation

$$\frac{1}{g(B)} \frac{\partial g}{\partial p}(B) = -\frac{L}{N}.$$

Thus,

$$\mathcal{Z}_N(L) \approx [g(B)]^N e^{LB}. \tag{2}$$

Hence the probability density for spacing r_1 between the particles 1 and 2 can be then reduced to the form

$$P(r_1) = \frac{\mathcal{Z}_{N-1}(L - r_1)}{\mathcal{Z}_N(L)} f(r_1).$$

Supposing $N \gg 1$ and using equation (2) we obtain

$$P(r_1) = \frac{1}{g(B)} f(r_1) e^{-Br_1},$$

which leads (after applying the same procedure for every pair of successive particles) to the distribution function for spacing r between arbitrary couple of neighbouring particles

$$P_\beta(r) = A e^{-\beta V(r)} e^{-Br} \quad (r \geq 0). \tag{3}$$

Note that constant A assures the normalization $\int_0^\infty P_\beta(r) dr = 1$. Furthermore, returning to the original choice $L = N$, the mean spacing is

$$\langle r \rangle \equiv \int_0^\infty r P_\beta(r) dr = 1. \tag{4}$$

The above two conditions can be understood as an equation system for unknown normalization constants A, B .

Let us proceed to the special variants of the gas studied. First, we draw our attention to the Coulomb gas with the logarithmic potential

$$V(r) := -\ln(r) \quad (r > 0).$$

Such a gas (usually called Dyson's gas, for example in [11]) is frequently used in many branches of physics (including the traffic research in [8]) and the corresponding spacing distribution reads as (see [1])

$$P_\beta(r) = \frac{(\beta + 1)^{\beta+1}}{\Gamma(\beta + 1)} r^\beta e^{-(\beta+1)r},$$

where $\Gamma(\xi)$ is the gamma function. Of larger physical interest, as demonstrated in [5] and [7], seem actually to be the potentials

$$V_\alpha(r) := r^{-\alpha} \quad (r > 0),$$

for $\alpha > 0$. The aim of the following computational procedure is to normalize the distribution

$$P_\beta(r) = A e^{-\frac{\beta}{r^\alpha}} e^{-Br}. \tag{5}$$

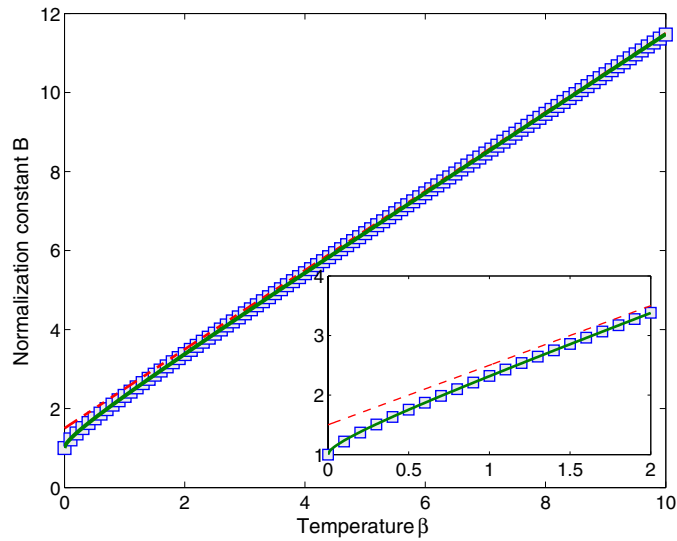


Figure 1. Normalization constant B depending on the inverse temperature β . Squares represent the exact value of B obtained from numerical computations. The dashed and solid curves display the large β approximation (10) and full approximation (8), respectively. The behaviour close to the origin is magnified in the inset.

Consider now the favourable choice $\alpha = 1$, for which the normalization integrals are exactly expressed as

$$\int_0^\infty e^{-\frac{\beta}{r}} e^{-Br} dr = 2\sqrt{\frac{\beta}{B}} \mathcal{K}_1(2\sqrt{\beta B}) \quad (6)$$

$$\int_0^\infty r e^{-\frac{\beta}{r}} e^{-Br} dr = 2\frac{\beta}{B} \mathcal{K}_2(2\sqrt{\beta B}), \quad (7)$$

where \mathcal{K}_λ is the Mac-Donald's function (the modified Bessel's function of the second kind) of order λ , having for $\lambda = 1$ and $\lambda = 2$ an approximate expression

$$\mathcal{K}_\lambda(y) = \sqrt{\frac{\pi}{2}} e^{-y} \left(y^{-1/2} + \frac{3}{8} 5^{\lambda-1} y^{-3/2} + \mathcal{O}(y^{-5/2}) \right).$$

Applying equations (6) and (7) to the normalization integrals one can determine the exact values of the constants A and B . Both of them can be, after applying Taylor's expansion procedure, very well estimated by the approximations

$$B \approx \beta + \frac{3 - e^{-\sqrt{\beta}}}{2}, \quad (8)$$

and

$$A \approx \frac{\sqrt{2\beta + 3 - e^{-\sqrt{\beta}}}}{\sqrt{8\beta} \mathcal{K}_1(\sqrt{4\beta^2 + 6\beta - 2\beta e^{-\sqrt{\beta}}})}. \quad (9)$$

Finally, we investigate the distribution (5) for general $\alpha > 0$. Although in this case the normalization integrals are not trivially solvable, the scaling (4) leads us to the simple approximate formula

$$B \approx \alpha\beta + 1 + \frac{\alpha}{2} \quad (\beta \gg 1). \quad (10)$$

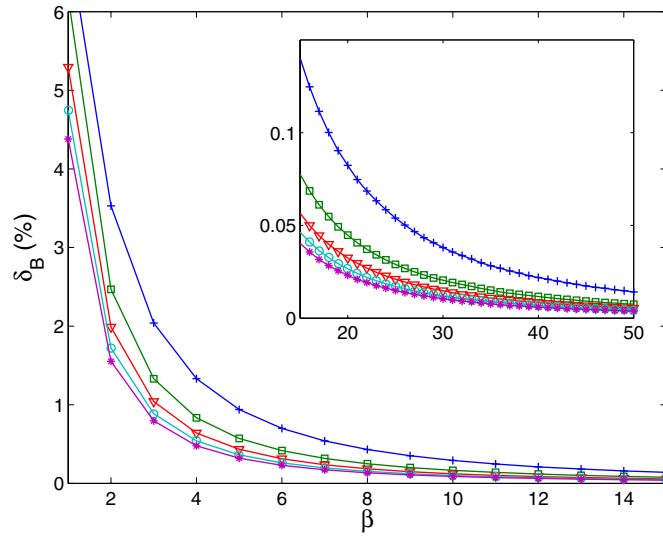


Figure 2. Relative deviation in the approximate value of the normalization constant B as a function of parameter β . We display the deviation (13) between the numerical value B_{ex} and the value B_{est} obtained from the large β approximation (10). The plus signs, squares, triangles, circles and stars correspond to the parameters $\alpha = 1, 2, 3, 4, 5$, respectively. The tails of the curves are magnified in the inset.

The large β estimation $r^{-\alpha} \approx 1 - \alpha + \alpha r^{-1}$, which holds true for values r around the mean distance $r \approx 1$, provides the asymptotical formula for the normalization constant A :

$$A \approx \frac{1}{2} \sqrt{1 + \frac{1}{2\beta} + \frac{1}{\alpha\beta} \frac{e^{\beta(1-\alpha)}}{\mathcal{K}_1(\sqrt{2\alpha\beta(2\alpha\beta + \alpha + 2)}}}. \tag{11}$$

For practical applications it seems to be useful to detect the critical inverse temperature β_{crit} under which the relative deviation between the exact (ex) and estimated (est) values of the constant A (or B)

$$\delta_{\log(A)} := \frac{|\log(A_{\text{ex}}) - \log(A_{\text{est}})|}{\log(A_{\text{ex}})} \tag{12}$$

$$\delta_B := \frac{|B_{\text{ex}} - B_{\text{est}}|}{B_{\text{ex}}} \tag{13}$$

are larger than the fixed acceptable deviation δ . For these purposes we plot the functional dependence $\delta_B = \delta_B(\beta)$ and $\delta_{\log(A)} = \delta_{\log(A)}(\beta)$ in figures 2 and 3, respectively. We note that the exact values $A_{\text{ex}}, B_{\text{ex}}$ were determined with the help of numerical computations.

Considering now the tested choice for the car-car potential $V(r) = r^{-1}$ we intend to compare the equilibrium distribution

$$P_\beta(r) = A e^{-\frac{\beta}{r}} e^{-Br} \tag{14}$$

with the relevant distributions of single-vehicle data measured continuously during approximately 140 days on the Dutch two-lane freeway A9. The macroscopic traffic density ϱ was calculated for samples of $N = 50$ subsequent cars passing a detector. For the purposes described above we divide the region of the measured densities $\varrho \in [0, 85 \text{ veh/km/lane}]$ into

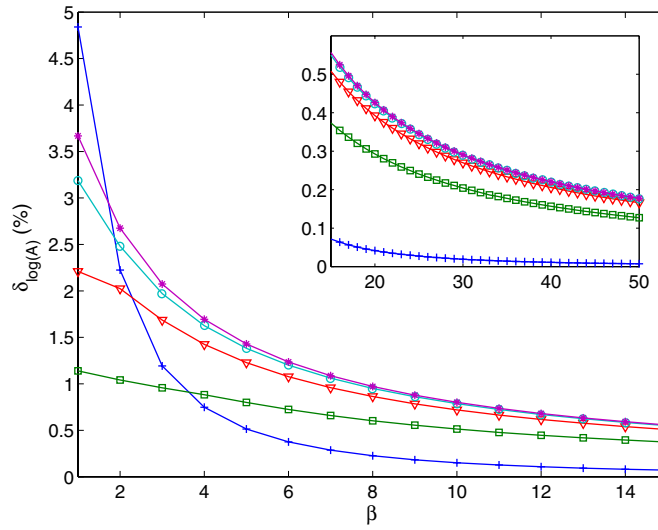


Figure 3. Relative deviation in the approximate value of the normalization constant A as a function of parameter β . Plotted is the deviation (12) between the numerically computed value A_{ex} and the estimated value (11). The symbols used here are consistent with the symbols in figure 2.

85 equidistant subintervals and separately analyse the data from each other. The sketched procedure prevents the undesired mixing of the states with a different inverse temperature β , i.e. with a different density. The bumper-to-bumper distance r_i among the succeeding cars (i th and $(i - 1)$ th) is calculated (after eliminating car-truck, truck-car, and truck-truck gaps) using the standard formula

$$r_i = v_i(t_i - t_{i-1}),$$

by means of netto time-headway $t_i - t_{i-1}$ and velocity v_i of the i th car (both directly measured with induction-loop detector) supposing that the velocity v_i remains constant between the times t_i, t_{i-1} when the i th car and the previous one are passing a measure point. Such a condition could be questionable, especially in the region of small densities where the temporal gaps are too large. However, the influence of a possible error is of marginal importance, as apparent from the fact that the distribution function plotted for small-density data does not show any visible deviation from Poisson behaviour expected for independent events (see figure 4 and relation (15)).

We note that mean distance among the cars is rescaled to 1 in all density regions. The thorough statistical analysis of the traffic data leads afterwards to the excellent agreement between clearance distribution computed from traffic data and formula (14) for the fitted value of inverse temperature β_{fit} (see figure 4). We have obtained the fit parameter β_{fit} by a least-square method, i.e. minimizing the error function χ^2 . The deviation χ^2 between the theoretical and empirical clearance distributions is plotted in figure 5 (low part).

Dimensionless inverse temperature β of the traffic sample, representing a quantitative description of mental strain under which the car-drivers are in a given situation, shows a non-trivial dependence on the traffic density ρ (as visible in figure 5(top part)). For free flow states ($\rho \lesssim 20$ veh/km/lane) one can recognize a rise in temperature having a linear behaviour (up to 10 veh/km/lane) and visible plateau above. In the intermediate region (between 20 and 50 veh/km/lane), where free traffic converts to the congested traffic, we detect a sharp increase in the first half. Such a behaviour can be simply elucidated by the fact that the drivers,

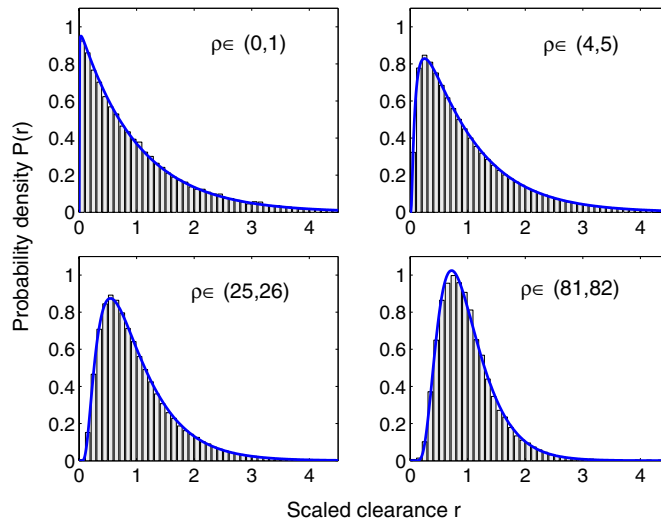


Figure 4. Probability density $P(r)$ for scaled spacing r between successive cars in traffic flow. Histograms represent the clearance distributions computed for traffic data from the indicated density region (in veh/km/lane). Note that the mean distance among the cars is rescaled to 1 in all density regions. The curves represent the predictions of statistical model (14) for the fitted value of inverse temperature β_{fit} . The respective values β_{fit} were carefully analysed and consecutively visualized in figure 5 (top part).

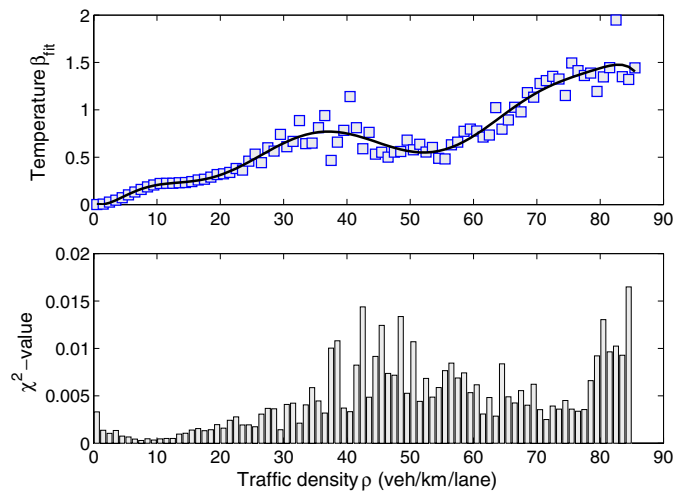


Figure 5. Inverse temperature β_{fit} and deviation χ^2 as a function of traffic density ρ . Squares stand for values of the fit parameter β_{fit} , for which the function (14) coincides with clearance distribution of traffic data. The curve represents a polynomial fit of relevant data. Bars from the lower part correspond to the sums of squared deviations between the empirical and the theoretical netto distance distributions for β_{fit} . We note that the value of the normalization constant B was determined via formula (8), because the values of the relevant inverse temperatures lie in the interval $[0, 2]$, where the linear approximation (10) is less suitable (see deviations in figure 2). The second normalization constant A was calculated by means of equation (9).

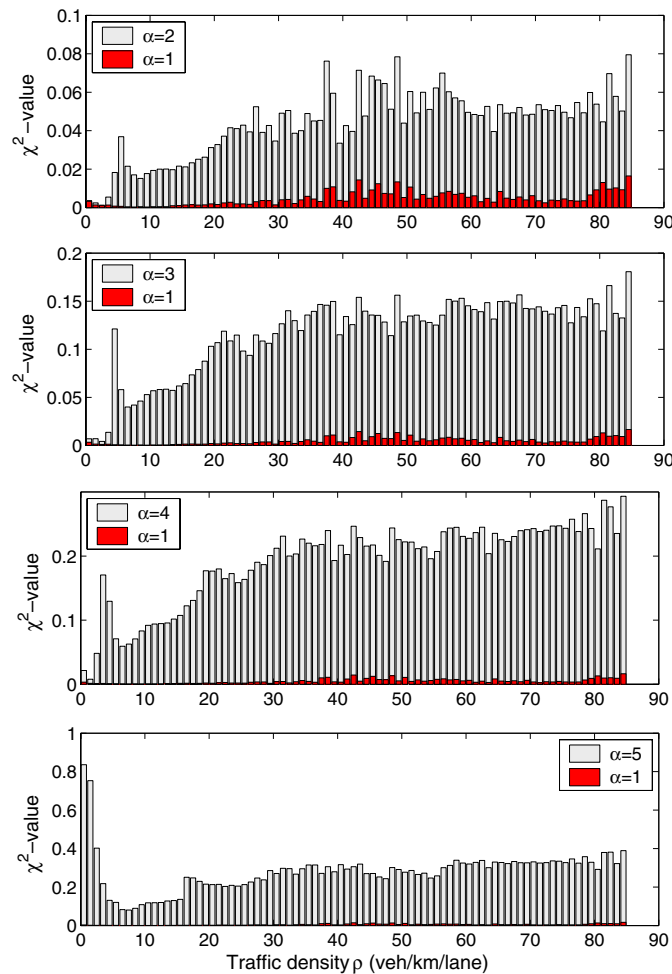


Figure 6. Deviation χ^2 between clearance distribution of cars moving in traffic stream and normalized distribution (5) evaluated for $\alpha = 2, 3, 4, 5$, respectively. Grey bars represent the sums of squared deviations depending on the traffic density for $\alpha = 2, 3, 4, 5$, respectively. Dark bars display the relevant deviations for $\alpha = 1$ previously plotted in figure 5 (lower part).

moving quite fast in a relatively dense traffic flow, are under a substantial psychological pressure, which finally results (for densities $\rho \in [35, 50]$ veh/km/lane) in the transition to the congested flows and therefore a drop in the inverse temperature. In a synchronized traffic regime ($\rho \gtrsim 50$ veh/km/lane) the driver's vigilance rapidly grows up which culminates the traffic-jam formation.

For completeness we have compared real-road clearance distributions with the probability density (5) specified for power-law potentials $V(r) = r^{-\alpha}$, where $\alpha = 2, 3, 4, 5$, respectively. A similar analysis was already introduced in [7]. From the careful analysis of statistical deviations χ^2 , comparisons between freeway data and the distribution (5), for $\alpha = 2, 3, 4, 5$, are substantially worse than those calculated for $\alpha = 1$ (follow figure 6). We emphasize that small deviations χ^2 (indicating a good agreement) detected near the origin in figure 6 are caused by the fact that for low traffic-densities the interactions among the cars are vanishing and the inter-vehicle gaps are therefore practically independent. The relevant distributions in

this case came close to the Poisson distribution (see the upper left-hand subplot of figure 4). However, the Poisson distribution can be obtained as a limit of distribution (3), i.e.

$$\lim_{\beta \rightarrow 0_+} P_\beta(r) = e^{-r}, \quad (15)$$

for the arbitrary function $V(r)$. For that reason it is impossible to detect the interaction potential in the traffic sample using the low density data only. The comparison of various potentials $V(r) = r^{-\alpha}$ (including the logarithmical potential $V(r) = -\ln(r)$) brings finally the message that interaction among the vehicles in traffic stream can be very well estimated by the short-ranged two-body power-law potential $V(r) = r^{-1}$. Predicted inter-vehicle-gap distributions correspond in this case to the computed probability density in all density intervals.

We append that another suitable quantity for comparison with single-vehicle data is a time-clearance distribution as well. Furthermore, time gaps among the succeeding cars are directly measurable and therefore not burden with errors caused by computation approximations. The determination of the exact form for time-headway probability density of the above thermodynamical traffic gas and relevant comparison with highway traffic data will be incorporated in the continuing work. Nevertheless, several analytical forms for the corresponding distribution have already been discussed in [5] and also in book [10].

To conclude we have found the analytical form of the thermal-equilibrium spacing distribution for a one-dimensional traffic gas which neighbouring particles are repulsed by the two-body potential $V = r^{-\alpha}$, where r is their mutual distance. The values of two normalization constants were successfully estimated by the convenient approximations. The calculated distribution (for $\alpha = 1$) with one free parameter (inverse temperature β) has been compared to the distance clearance distribution of the freeway traffic samples with an excellent outcome. It was demonstrated that the inverse temperature of the traffic sample non-trivially depends on the traffic density. The obtained agreement between experimental and calculated distributions confirms a convenience of the traffic potential used for description of local traffic interactions. This paper crowns the quest for the mathematical formula for probability density of mutual clearances among the cars in a traffic stream and supports the possibility for applying the equilibrium statistical physics to traffic modelling.

Acknowledgments

We would like to thank the Dutch Ministry of Transport for providing the single-vehicle induction-loop-detector data. This work was supported by the Ministry of Education, Youth and Sports of the Czech Republic within the project LC06002.

References

- [1] Bogomolny E B, Gerland U and Schmit C 2001 *Eur. Phys. J. B* **19** 121
- [2] Helbing D 2001 *Rev. Mod. Phys.* **73** 1067
- [3] Helbing D and Treiber M 2003 *Preprint cond-mat/0307219*
- [4] Helbing D and Treiber M 1998 *Phys. Rev. Lett.* **81** 3042
- [5] Helbing D, Treiber M and Kesting A 2006 *Physica A* **363** 62
- [6] Neubert L, Santen L, Schadschneider A and Schreckenberg M 1999 *Phys. Rev. E* **60** 6480
- [7] Krbalek M and Helbing D 2004 *Physica A* **333** 370
- [8] Krbalek M, Seba P and Wagner P 2001 *Phys. Rev. E* **64** 066119
- [9] Mahnke R, Hinkel J, Kaupužs J and Weber H 2006 *Preprint cond-mat/0606509*
- [10] May A D 1990 *Traffic Flow Fundamentals* (Englewood Cliffs, NJ: Prentice Hall)
- [11] Scharf R and Izrailev F M 1990 *J. Phys. A: Math. Gen.* **23** 963